AIAA JOURNAL
Vol. 32, No. 10, October 1994

Finite Element Time Domain—Modal Formulation for Nonlinear Flutter of Composite Panels

R. C. Zhou,* David Y. Xue,† and Chuh Mei‡
Old Dominion University, Norfolk, Virginia 23529

A finite element time domain modal approach is presented for determining the nonlinear flutter characteristics of composite panels at elevated temperatures. The von Kármán large-deflection strain-displacement relations, quasisteady first-order piston theory aerodynamics, and quasisteady thermal stress theory are used to formulate the nonlinear panel flutter finite element equations of motion in nodal displacements. A set of nonlinear modal equations of motion of much smaller degrees of freedom for the facilitation in time numerical integration is then obtained through a modal transformation and reduction. All five types of panel behavior—flat, buckled, limit-cycle, periodic, and chaotic motions—can be determined. Examples show the accuracy, convergence, and versatility of the present approach.

Nomenclature

$[A]$, $[B]$, $[D]$	= extension, coupling, and bending laminate stiffness matrices
a, b	= panel length and width
$[C]$	= modal aerodynamic damping matrix
E_1, E_2	= Young's moduli in major and minor axes
G_{12}	= shear modulus
h	= panel thickness
$[K]$, $[k]$	= system and element linear stiffness matrices
$[K1]$, $[k1]$	= first-order nonlinear stiffness matrices
$[K2]$, $[k2]$	= second-order nonlinear stiffness matrices
$[M]$, $[m]$	= mass matrices
M_∞	= Mach number
p_a	= aerodynamic pressure
$\{q\}$	= modal amplitude vector
u, v	= in-plane displacements
w	= panel deflection
α_1, α_2	= major and minor coefficients of thermal expansion
ΔT	= temperature change
$\{\varepsilon\}$	= total strain vector
θ	= lamination angle
$\{\kappa\}$	= curvature vector
λ	= nondimensional aerodynamic pressure
μ	= air-panel mass ratio
ν	= Poisson's ratio
ρ	= mass density
$\{\sigma\}$	= stress vector
τ	= nondimensional time
$[\Phi]$	= modal matrix
$\{\phi\}$	= normal modes
ω_0	= reference frequency

Subscripts

a	= air
b	= bending
cr	= critical
m	= membrane
ref	= reference

Superscripts

r, s	= rth and sth normal modes
t	= transpose

Introduction

PANEL flutter has been encountered in the operation of aircraft and missiles at supersonic speed. Panel flutter differs from the conventional lifting surface or wing flutter in at least three aspects: 1) it is a transonic/supersonic phenomenon; 2) the airflow is only on one side of the panel; and 3) the large-deflection structural nonlinearities tend strongly to exhibit limit-cycle oscillations. The earliest reported structural failures that can be attributed to panel flutter were the failure of the 60–70 early German V-2 rockets during World War II.[1] A most recent structural failure due to panel flutter (and also acoustic fatigue) was reported at the AIAA 1992 Dynamics Specialists Conference.[2] After the flight tests of the F-117A stealth fighter, cracks were found in about half of the laminated composite skin panels. Those panels were then redesigned and stiffened.

Panel flutter has received resurgent interest due to the development of high-speed flight vehicles such as the YF-22, High Speed Civil Transport, and National Aero-Space Plane (NASP). To properly analyze and design an aircraft or missile structure that is traveling at high supersonic speeds, the effects of temperature as well as aerodynamic pressure must be considered. The friction from the surrounding air causes increased heating of the structure. The presence of high thermal loads usually results in flutter motions at dynamic pressures lower than when there are no temperature effects. An excellent summary of both linear and nonlinear panel flutter research through 1970 was given by Dowell.[3] Reed et al.[4] conducted a survey in the area of hypersonic flutter in support of the NASP program. Gray and Mei[5] recently gave a complete survey on various theoretical considerations and analytical methods for nonlinear panel flutter up to 1991.

Very few investigations on panel flutter have dealt with thermal effects.[6–12] Houbolt[6] was the first who studied the flutter boundaries for two-dimensional panels with uniform temperature distribution. The panel deflection due to the combined aerodynamic pressure and thermal loads was assumed to consist of two components: a thermal postbuckling deflection with the influence of dynamic pressure and a time-dependent flutter deflection. Two linear natural vibration modes were used for the postbuckling deflection that was considered to be large in the von Kármán sense. The dynamic flutter deflection was considered to be small. Thus, nonlin-

Received Dec. 17, 1993; revision received April 4, 1994; accepted for publication April 4, 1994; presented as Paper 94-1424 at the AIAA/ASME/ASCE/AHS/ASC 35th Structures, Structural Dynamics, and Materials Conference, Hilton Head, SC, April 18–20, 1994.

*Graduate Research Assistant, Department of Aerospace Engineering. Student Member AIAA.

†Research Associate, Department of Aerospace Engineering. Member AIAA.

‡Professor, Department of Aerospace Engineering. Associate Fellow AIAA.

ear thermal postbuckling including the effects of airflow and linear panel flutter including the thermal effects were investigated. Buckling stability and flutter boundaries were obtained for two-dimensional panels of pinned ends and clamped ends.

Application of the finite element methods to study linear flutter of thermally buckled two-dimensional panels was reported by Yang and Han[8] for uniform temperature and by Xue et al.[9] for nonuniform temperature $\Delta T(x)$ distribution. Extension of the finite element method to nonlinear panel flutter with temperature effects was given by Xue and Mei[10,11] for two-dimensional and three-dimensional isotropic panels of arbitrary shape and by Dixon and Mei[12] for rectangular composite panels.

As disclosed in all of those surveys, the aerodynamic theory employed for the most part for panel flutter at high supersonic Mach number ($M_\infty > 1.6$) is the quasisteady first-order piston theory aerodynamics. Classical continuum approaches of nonlinear panel flutter are determined usually through the use of Galerkin's method in the spatial domain and then in the temporal domain by direct numerical integration[3,13] in general, or by such techniques as perturbation, and harmonic balance (see Refs. 3 and 5). In nonlinear panel flutter investigations using the finite element frequency domain (FE-FD) formulation,[5,8–12,14] the linearized updated mode with a nonlinear time function approximation (LUM/NTF) method [5,9–12] is usually employed. As it was concluded in Ref. 11, the FE-FD method can determine the buckling and flutter stability boundaries and the harmonic limit-cycle motions in the dynamic pressure vs temperature (λ vs $\Delta T/\Delta T_{cr}$) plot shown in Fig. 1. However, the FE-FD method can give no information at all in the region of nonharmonic and chaotic motions (area ABE).

This paper presents a finite element time domain modal (FE-TM) formulation for the nonlinear flutter analysis of thin arbitrarily laminated composite panels at elevated temperatures. Thus, all five types of panel behavior—flat, buckled, limit-cycle oscillations, periodic but nonharmonic, and chaotic motions—can be determined using the FE-TM method. To validate the accuracy of the FE-TM approach, limit-cycle motions at $\Delta T/\Delta T_{cr} = 0$, 1, and 2 are obtained for a simply supported square isotropic panel, and results are compared with solutions from the FE-FD[11] and classical continuum Galerkin/numerical integration[3,13] methods. For the modal reduction, the number of modes for a converged limit-cycle amplitude of a composite panel is studied. To demonstrate the versatility of the FE-TM method, limit-cycle, periodic, and chaotic motions are presented for isotropic and composite panels at certain combinations of dynamic pressure and thermal load.

Nonlinear Panel Flutter Formulation

Constitutive and Strain-Displacement Relations

The von Kármán strain-displacement relations for a plate undergoing extension and bending at any point z through the thickness is the sum of membrane and change of curvature strain components as

$$\{\varepsilon\} = \begin{Bmatrix} \varepsilon_x \\ \varepsilon_y \\ \gamma_{xy} \end{Bmatrix} = \{\varepsilon^0\} + z\{\kappa\} = \{\varepsilon_m^0\} + \{\varepsilon_\theta^0\} + z\{\kappa\}$$

$$= \begin{Bmatrix} u_{,x} \\ v_{,y} \\ u_{,y} + v_{,x} \end{Bmatrix} + \frac{1}{2}\begin{Bmatrix} w_{,x}^2 \\ w_{,y}^2 \\ 2w_{,x}w_{,y} \end{Bmatrix} + z\begin{Bmatrix} -w_{,xx} \\ -w_{,yy} \\ -2w_{,xy} \end{Bmatrix} \tag{1}$$

The stress-strain relations for a general kth orthotropic lamina having a lamination angle θ, subjected to a temperature change of $\Delta T(x, y, z)$, are

$$\{\sigma\}_k = \begin{Bmatrix} \sigma_x \\ \sigma_y \\ \tau_{xy} \end{Bmatrix}_k = \begin{bmatrix} \bar{Q}_{11} & \bar{Q}_{12} & \bar{Q}_{16} \\ \bar{Q}_{12} & \bar{Q}_{22} & \bar{Q}_{26} \\ \bar{Q}_{16} & \bar{Q}_{26} & \bar{Q}_{66} \end{bmatrix}_k \left(\{\varepsilon\} - \begin{Bmatrix} \alpha_x \\ \alpha_y \\ \alpha_{xy} \end{Bmatrix}_k \Delta T \right) \tag{2}$$

where $[\bar{Q}]$ is the transformed reduced stiffness matrix.

The stress resultants, per unit length, are defined as

$$(\{N\}, \{M\}) = \int_{-h/2}^{h/2} \{\sigma\}_k (1, z)\, dz \tag{3}$$

This leads to the constitutive relations for a composite laminate

$$\begin{Bmatrix} N \\ M \end{Bmatrix} = \begin{bmatrix} A & B \\ B & D \end{bmatrix} \begin{Bmatrix} \varepsilon^0 \\ \kappa \end{Bmatrix} - \begin{Bmatrix} N_{\Delta T} \\ M_{\Delta T} \end{Bmatrix} \tag{4}$$

where the thermal forces and moments are

$$(\{N_{\Delta T}\}, \{M_{\Delta T}\}) = \int_{-h/2}^{h/2} [\bar{Q}]_k \{\alpha\}_k \Delta T(1, z)\, dz \tag{5}$$

Aerodynamic Pressure Function

As disclosed in all of the panel flutter surveys, the aerodynamic theory employed for panel flutter at high supersonic speeds ($M_\infty > 1.6$) is the quasisteady first-order piston aerodynamics. The aerodynamic pressure is represented as

$$p_a = -\frac{2q_a}{\beta}\left(w_{,x} + \frac{M_\infty^2 - 2}{M_\infty^2 - 1}\frac{1}{V_\infty} w_{,t} \right)$$

$$= -\left(\lambda \frac{D_{110}}{a^3} w_{,x} + \frac{g_a}{\omega_0}\frac{D_{110}}{a^4} w_{,t} \right) \tag{6}$$

where $q_a = \rho_a V_\infty^2/2$ is the dynamic pressure, ρ_a the air density, V_∞ the airflow speed, a the panel length, $\omega_0 = (D_{110}/\rho h a^4)^{1/2}$ a convenient reference frequency, and $\beta = (M_\infty - 1)^{1/2}$. The value D_{110} is the first entry of the bending stiffness matrix $[D]$ calculated when all of the fibers of the composite layers are aligned in the direction of the airflow (x axis). The nondimensional dynamic pressure and aerodynamic damping are given by

$$\lambda = \frac{2q_a a^3}{\beta D_{110}}, \qquad g_a = \frac{\rho_a V_\infty (M_\infty^2 - 2)}{\rho h \omega_0 \beta^3} \tag{7}$$

Other commonly used nondimensional parameters are the air-panel mass ratio and aerodynamic damping coefficient; they are defined as

$$\mu = \frac{\rho_a a}{\rho h}, \qquad c_a = \left(\frac{M_\infty^2 - 2}{M_\infty^2 - 1} \right)^2 \frac{\mu}{\beta} \tag{8}$$

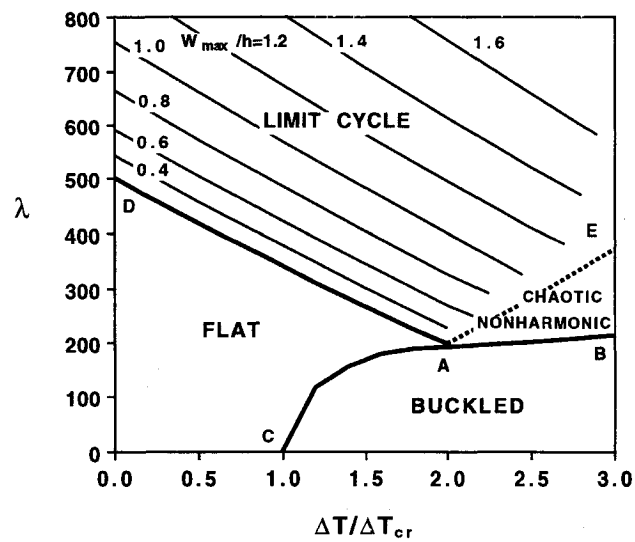

Fig. 1 Stability boundaries and limit-cycle amplitudes of a simply supported square isotropic panel with uniform temperature.

From Eqs. (7) and (8), $g_a = (\lambda c_a)^{1/2}$ and $c_a \approx \mu/M_\infty$ (for $M_\infty \gg 1$) as used in Refs. 3 and 13.

Finite Element Equations of Motion

Proceeding from this point, the displacements in Eq. (1) are approximated over a typical element, e.g., rectangular[5,12] and triangular,[11,14] using the corresponding interpolation functions and nodal displacements. Through the use of Hamilton's principle and finite element expression, the equations of motion for a laminated composite plate element, rectangular[12] or triangular,[11] subjected to dynamic pressure λ and temperature change $\Delta T(x, y, z)$ simultaneously can be written as

$$\frac{1}{\omega_0^2}\begin{bmatrix}[m]_b & 0\\ 0 & [m]_m\end{bmatrix}\begin{Bmatrix}\ddot{w}_b\\ \ddot{w}_m\end{Bmatrix} + \frac{g_a}{\omega_0}\begin{bmatrix}[g] & 0\\ 0 & 0\end{bmatrix}\begin{Bmatrix}\dot{w}_b\\ \dot{w}_m\end{Bmatrix}$$
$$+\left(\lambda\begin{bmatrix}[a_a] & 0\\ 0 & 0\end{bmatrix} + \begin{bmatrix}[k]_b & [k_B]\\ [k_B]^t & [k]_m\end{bmatrix} - \begin{bmatrix}[k_{N\Delta T}] & 0\\ 0 & 0\end{bmatrix}\right.$$
$$\left.+\begin{bmatrix}[k1_{Nm}] + [k1_{NB}] & [k1]_{bm}\\ [k1]_{mb} & 0\end{bmatrix} + \begin{bmatrix}[k2] & 0\\ 0 & 0\end{bmatrix}\right)\begin{Bmatrix}w_b\\ w_m\end{Bmatrix}$$
$$= \begin{Bmatrix}\{p_{\Delta T}\}_b\\ \{p_{\Delta T}\}_m\end{Bmatrix} \tag{9}$$

where $[m]$, $[g]$, $[a_a]$, and $[k]$ are the element mass, aerodynamic damping, aerodynamic influence, and linear stiffness matrices, respectively; $[k1]$ and $[k2]$ depend linearly and quadratically upon the element displacements $\{w\}$, respectively; and $\{p_{\Delta T}\}$ is the element thermal load vector. The subscripts B, $N\Delta T$, Nm, and NB denote that the corresponding stiffness matrix is due to the laminate coupling stiffness $[B]$, thermal membrane forces $\{N_{\Delta T}\}$, membrane force components $\{N_m\}(=[A]\{\varepsilon_m^0\})$, and $\{N_B\}(=[B]\{\kappa\})$, respectively. All element matrices in Eq. (9) are symmetric except the aerodynamic influence matrix $[a_a]$, which is skew symmetric. Detailed derivation of the element equations of motion and expressions of the element matrix are included in Refs. 5, 9, and 12.

After assembling the individual finite elements for the complete panel and applying the kinematic boundary conditions, the system equations of motion for a given laminated composite panel of general planform subjected to a combined airflow and temperature can be expressed in the matrix form as

$$\frac{1}{\omega_0^2}\begin{bmatrix}[M]_b & 0\\ 0 & [M]_m\end{bmatrix}\begin{Bmatrix}\ddot{W}_b\\ \ddot{W}_m\end{Bmatrix} + \frac{g_a}{\omega_0}\begin{bmatrix}[G] & 0\\ 0 & 0\end{bmatrix}\begin{Bmatrix}\dot{W}_b\\ \dot{W}_m\end{Bmatrix}$$
$$+\left(\lambda\begin{bmatrix}[A_a] & 0\\ 0 & 0\end{bmatrix} + \begin{bmatrix}[K]_b & [K_B]\\ [K_B]^t & [K]_m\end{bmatrix} - \begin{bmatrix}[K_{N\Delta T}] & 0\\ 0 & 0\end{bmatrix}\right.$$
$$\left.+\begin{bmatrix}[K1_{Nm}] + [K1_{NB}] & [K1]_{bm}\\ [K1]_{mb} & 0\end{bmatrix} + \begin{bmatrix}[K2] & 0\\ 0 & 0\end{bmatrix}\right)\begin{Bmatrix}W_b\\ W_m\end{Bmatrix}$$
$$= \begin{Bmatrix}\{P_{\Delta T}\}_b\\ \{P_{\Delta T}\}_m\end{Bmatrix}$$

or simply

$$\frac{1}{\omega_0^2}[M]\{\ddot{W}\} + \frac{g_a}{\omega_0}[G]\{\dot{W}\} + (\lambda[A_a] + [K] - [K_{N\Delta T}]$$
$$+ [K1] + [K2])\{W\} = \{P_{\Delta T}\} \tag{10}$$

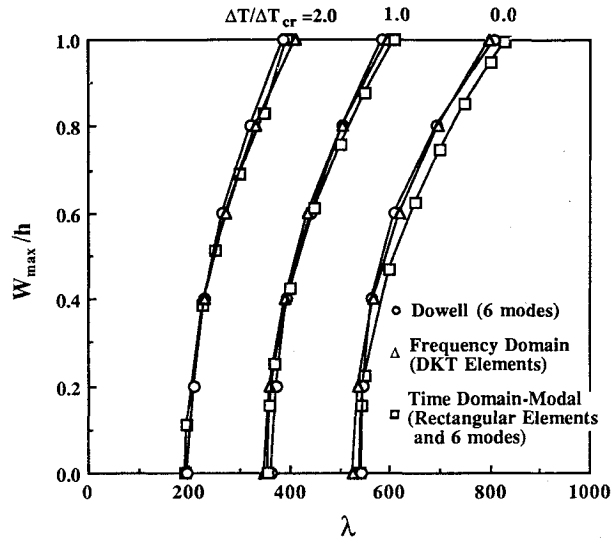

Fig. 2 Comparison of limit-cycle amplitudes for a simply supported square isotropic panel ($\mu/M_\infty = 0.1$).

The system equations of motion for nonlinear flutter of composite panels at elevated temperatures are thus obtained. Two methods, frequency domain and time domain, can be used to determine panel flutter response from Eq. (10). The FE-FD method consists of two solution steps in sequence. In the first step, the thermal postbuckling panel deflection with the influence of dynamic pressure is determined using the Newton-Raphson iteration technique. The limit-cycle oscillations are determined in the second step using the LUM/NTF method.[5,9–12] The FE-FD method,[5,10–12] which has been used successfully to study nonlinear panel flutter, requires less computational time[15] than the method of time numerical integration. However, the FE-FD method cannot predict the periodic and chaotic panel motions. Detailed descriptions of the FE-FD formulation and the LUM/NTF method are given in Refs. 5, 11, and 12.

Time Domain Modal Method

Modal Reduction

The system equations of motion presented in Eq. (10) are not suitable for numerical integration because of two shortcomings: 1) the number of degrees of freedom of the system nodal displacement vector $\{W\}$ is too large, and 2) the nonlinear stiffness matrices are functions of the system displacement vector. Therefore, Eq. (10) has to be transformed into a set of properly chosen modal coordinates with rather small degrees of freedom (<10, and 6 modes by Dowell[3]). This is accomplished by a modal transformation

$$\{W\} = \sum_{r=1}^{n}\sum_{s=1}^{m} q_{rs}(t)\{\phi_{rs}\} \tag{11}$$

where $\{\phi_{rs}\}$ corresponds to the normal mode (r, s) from the linear vibration solution of the system

$$\omega_{rs}^2[M]\{\phi_{rs}\} = [K]\{\phi_{rs}\} \tag{12}$$

For a rectangular panel with airflow along its length, the proper modes are the first few in the airflow freestream direction and the first mode ($m = 1$) in the spanwise direction. Equation (11) thus becomes

$$\{W\} = \sum_{r=1}^{n} q_r(t)\{\phi_r\} = [\Phi]\{q\} \tag{13}$$

Nonlinear Modal Stiffness Matrices and Modal Equations

The formulation of the system equations of motion in terms of modal coordinates necessitates the transformation of the individual matrices in Eq. (10) to their equivalent modal matrices. The nonlinear stiffness matrices, $[K1]$ and $[K2]$, can be expressed in terms of the modal coordinates as

$$[K1] = \sum_{r=1}^{n} q_r [K1]^{(r)} \tag{14}$$

and

$$[K2] = \sum_{r=1}^{n}\sum_{s=1}^{n} q_r q_s [K2]^{(rs)} \tag{15}$$

The nonlinear modal stiffness matrices, $[K1]^{(r)}$ and $[K2]^{(rs)}$, are evaluated with the corresponding element components [see Eq. (9)] obtained from the system modes $\{\phi_r\}$ and $\{\phi_s\}$ as

$$[K1]^{(r)} = \sum_{\text{all elements}} \begin{bmatrix} [k1_{Nm}]^{(r)} + [k1_{NB}]^{(r)} & [k1]^{(r)}_{bm} \\ [k1]^{(r)}_{mb} & 0 \end{bmatrix} \tag{16}$$

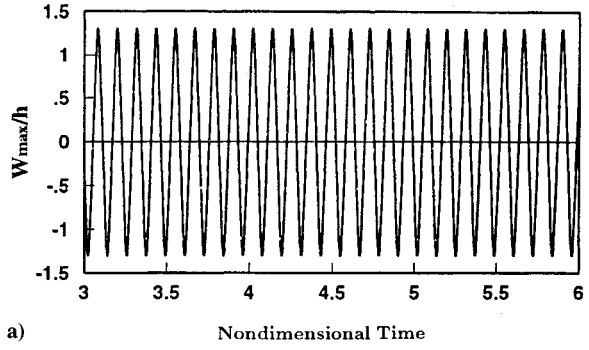

a)

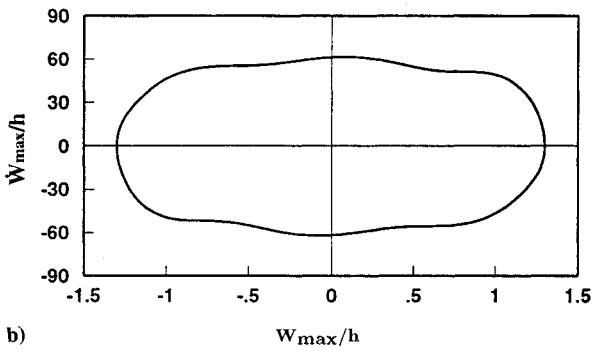

b)

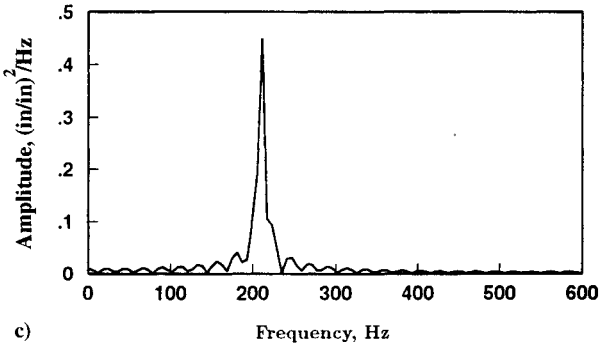

c)

Fig. 3 Limit-cycle motions of a simply supported square isotropic panel ($\mu/M_\infty = 0.1$) at $\lambda = 800$ and $\Delta T/\Delta T_{cr} = 1.0$.

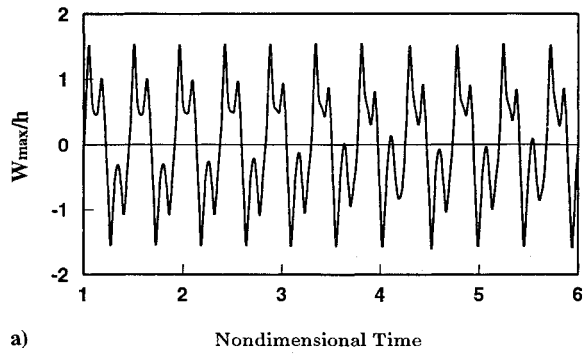

a)

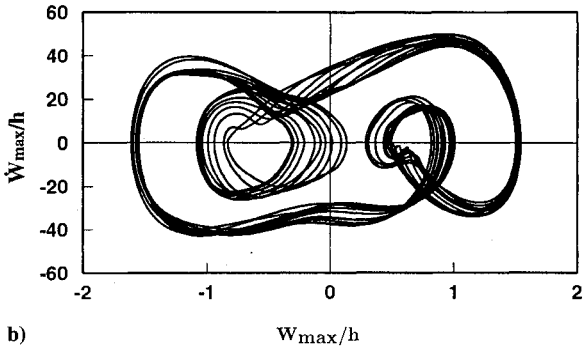

b)

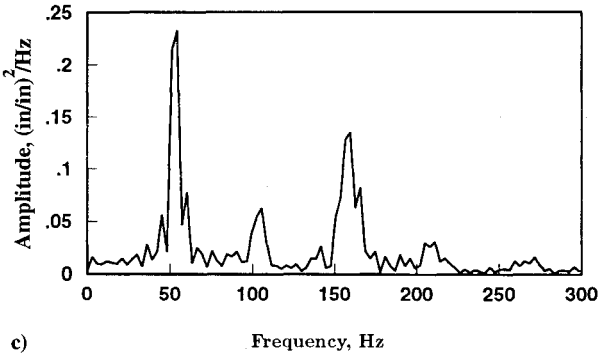

c)

Fig. 4 Periodic motions of a simply supported square isotropic panel ($\mu/M_\infty = 0.1$) at $\lambda = 300$ and $\Delta T/\Delta T_{cr} = 3.0$.

and

$$[K2]^{(rs)} = \sum_{\text{all elements}} \begin{bmatrix} [k2]^{(rs)} & 0 \\ 0 & 0 \end{bmatrix} \tag{17}$$

Thus, all entries of the nonlinear modal stiffness matrices, $[K1]^{(r)}$ and $[K2]^{(rs)}$, are known quantities.

With the modal transformation of Eq. (13) and nonlinear modal stiffness matrices in Eqs. (14) and (15), the system equations of motion, Eq. (10), are thus transformed to the general Duffing equation in reduced modal coordinates as

$$[\bar{M}]\{q_{,\tau\tau}\} + [C]\{q_{,\tau}\} + ([\bar{K}] + [K_q] + [K_{qq}])\{q\} = \{f\} \tag{18}$$

where $\tau = \omega_0 t$ is the nondimensional time, and the modal mass $[\bar{M}]$ and modal aerodynamic damping $[C]$ matrices are diagonal as

$$([\bar{M}], [C]) = [\Phi]^t([M], g_a[G])[\Phi] \tag{19}$$

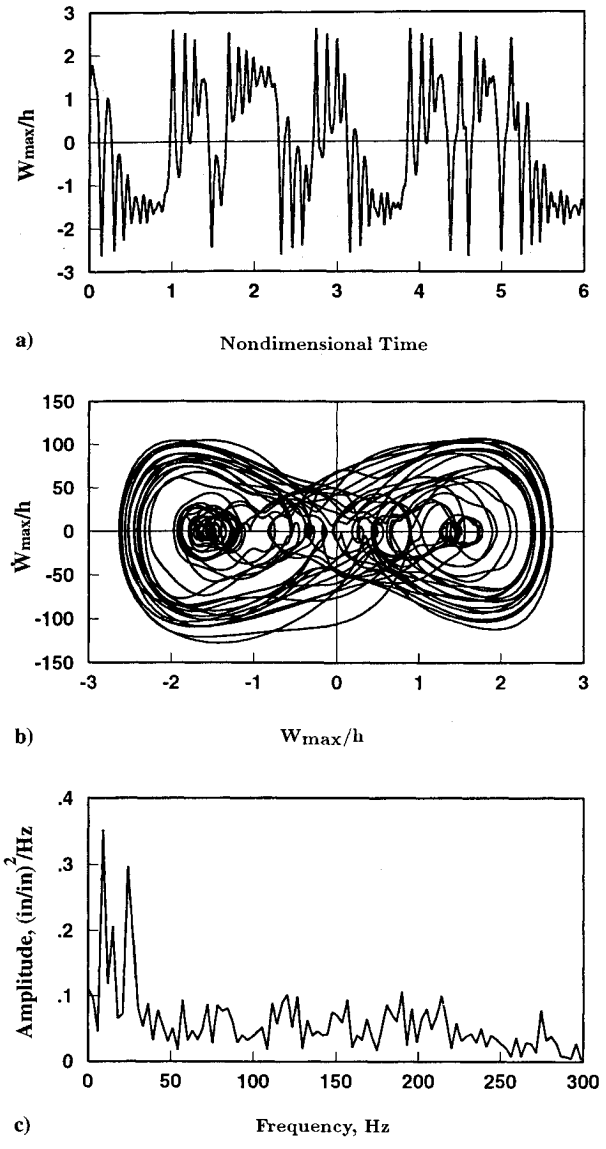

Fig. 5 Chaotic motions of a simply supported square isotropic panel ($\mu/M_\infty = 0.1$) at $\lambda = 300$ and $\Delta T/\Delta T_{cr} = 6.0$.

the linear terms in $\{q\}$ are

$$[\bar{K}]\{q\} = [\Phi]^t(\lambda[A_a] + [K] - [K_{N\Delta T}])[\Phi]\{q\} \quad (20)$$

and the quadratic and cubic terms in $\{q\}$ are

$$[K_q]\{q\} = [\Phi]^t\left(\sum_{r=1}^{n} q_r[K1]^{(r)}\right)[\Phi]\{q\} \quad (21)$$

and

$$[K_{qq}]\{q\} = [\Phi]^t\left(\sum_{r=1}^{n}\sum_{s=1}^{n} q_r q_s[K2]^{(rs)}\right)[\Phi]\{q\} \quad (22)$$

and the modal thermal load vector is

$$\{f\} = [\Phi]^t\{P_{\Delta T}\} \quad (23)$$

For symmetrically laminated composite and isotropic ($[B] = 0$) panels, the bending $\{\phi_r\}_b$ and membrane $\{\phi_r\}_m$ mode shapes in Eq. (13) are uncoupled. Thus, a properly chosen modal transformation will have the form

$$\{W_b\} = \sum_{r=1}^{n} q_r(t)\{\phi_r\}_b = [\Phi]\{q\} \quad (24)$$

where $\{\phi_r\}_b$ is the normal mode from

$$\omega_r^2[M]_b\{\phi_r\}_b = [K]_b\{\phi_r\}_b \quad (25)$$

and the system equations of motion for symmetric composite and isotropic panels are reduced to the Duffing equation as

$$[\bar{M}]_b\{q_{,\tau\tau}\} + [C]\{q_{,\tau}\} + ([\bar{K}]_b + [K_{qq}]_b)\{q\} = \{f\} \quad (26)$$

The detailed expressions of the diagonal modal mass $[\bar{M}]_b$, diagonal modal aerodynamic damping $[C]$, linear modal stiffness $[\bar{K}]_b$, and second-order nonlinear modal stiffness $[K_{qq}]_b$, matrices are given in the Appendix.

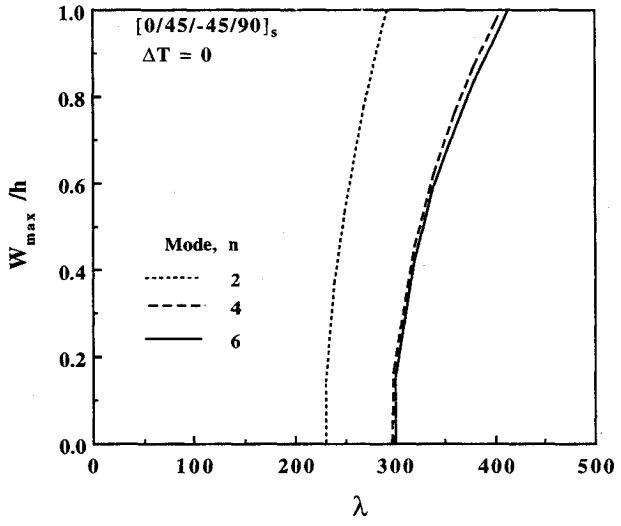

Fig. 6 Convergence of limit-cycle amplitudes for a simply supported square $[0/45/-45/90]_s$ panel ($\mu/M_\infty = 0.01$).

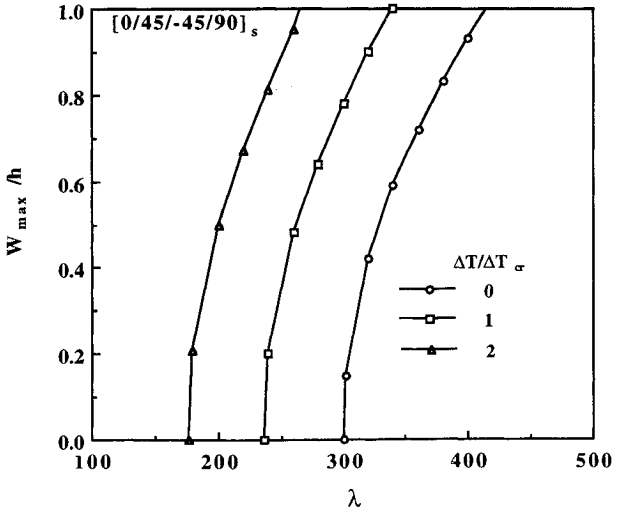

Fig. 7 Effect of temperature on limit-cycle amplitude for a simply supported square $[0/45/-45/90]_s$ panel ($\mu/M_\infty = 0.01$).

For various combinations of dynamic pressure λ, temperature change ΔT and aerodynamic damping $g_a(\approx \sqrt{\lambda\mu/M_\infty})$, all five types of panel behavior—flat, buckled, limit-cycle, periodic, and chaotic motions—can be determined from the nonlinear modal equations of motion, Eq. (18) or Eq. (26), using any numerical integration scheme such as the Runge-Kutta or Newmark-β method.

Results and Discussions

Isotropic Panel

To verify the present finite element time domain modal formulation, the limit-cycle results are obtained for a simply supported isotropic square plate with $\mu/M_\infty = 0.1$, at $\Delta T/\Delta T_{cr} = 0$, 1.0, and 2.0 shown in Fig. 2. The temperature distribution ΔT is assumed to be constant in all of the examples. Because of the symmetry in airflow direction, a half-plate is modeled by using a 12×3 mesh or 36 rectangular plate elements, and the finite element system equations of motion are reduced to six nonlinear modal equations in the form of Eq. (26). Limit-cycle results by Dowell[3] using a six-mode model and by FE-FD using 48 discrete Kirchhoff triangular (DKT) elements (half-plate with $8 \times 3 \times 2$ mesh) are also shown in Fig. 2 for comparison. It demonstrates excellent agreement of these three methods.

The limit-cycle amplitude vs nondimensional time τ, the phase plane plot of $\dot{w}_{max}/h$ vs w_{max}/h, and the power spectral density

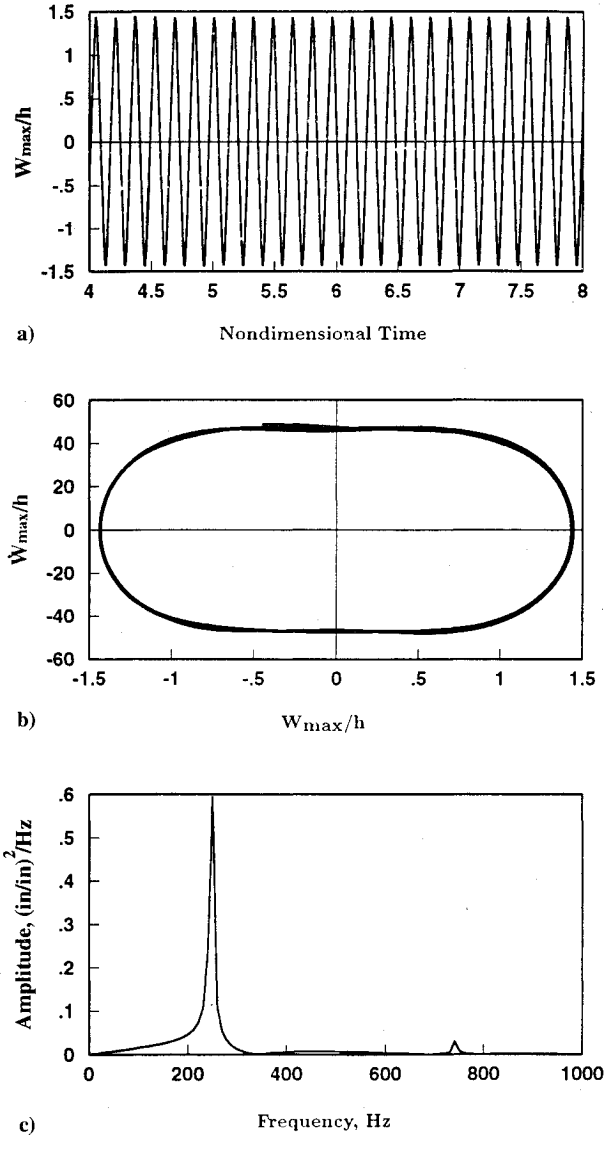

Fig. 8 Limit-cycle motions of a simply supported square [0/45/–45/90]$_s$ panel ($\mu/M_\infty = 0.01$) at $\lambda = 450$ and $\Delta T/\Delta T_{cr} = 1.0$.

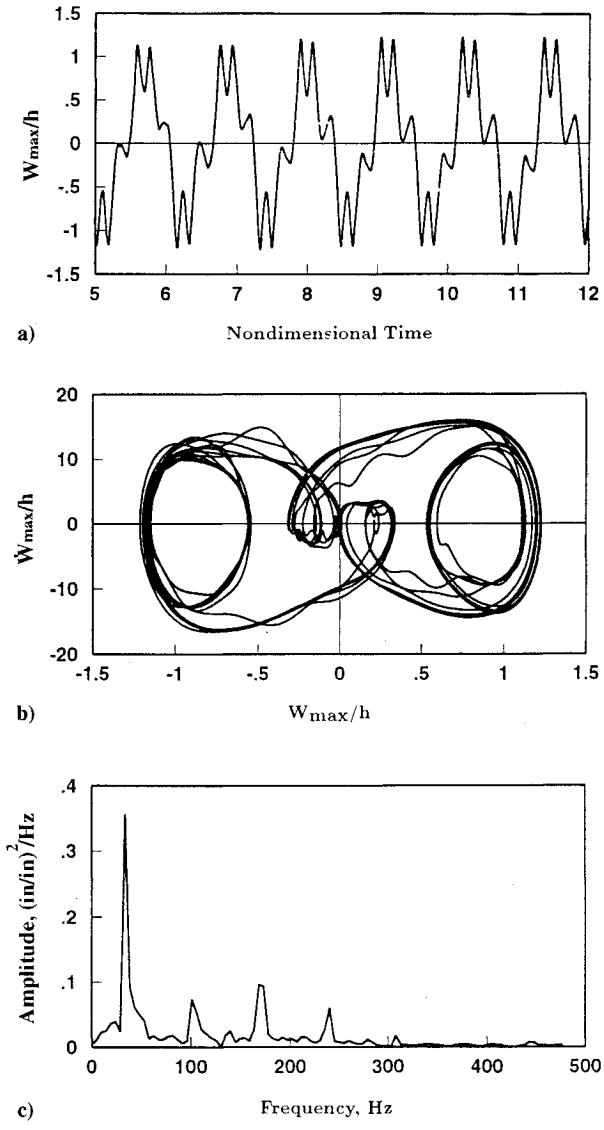

Fig. 9 Periodic motions of a simply supported square [0/45/–45/90]$_s$ panel ($\mu/M_\infty = 0.01$) at $\lambda = 140$ and $\Delta T/\Delta T_{cr} = 3.0$.

(PSD) of w_{max}/h are shown in Figs. 3a–3c for a simply supported isotropic square plate at $\lambda = 800$ and $\Delta T/\Delta T_{cr} = 1.0$. The time history in Fig. 3a describes a harmonic limit-cycle motion, and the phase plane plot and the PSD verify that the panel motion is dominated by a simple harmonic motion.

The same simply supported panel at $\lambda = 300$ and $\Delta T/\Delta T_{cr} = 3.0$ exhibits periodic motions as shown in Figs. 4a–4c. As can be seen, the results in Fig. 4c show three frequencies dominating the power spectrum, which is the expected result for a periodic motion with three dominant orbits in the phase plane plot (Fig. 4b). The limit-cycle and the periodic motions are both independent on the initial conditions. The response figures shown in Figs. 3a and 4a are the steady-state response after the transients have decayed.

At moderate $\lambda = 300$ and large temperature ratio $\Delta T/\Delta T_{cr} = 6.0$, the simply supported panel motion is expected to be chaotic as shown in Figs. 5a–5c. The time history in Fig. 5a shows clearly snap-through (or oil-canning) motions of the panel. The PSD (Fig. 5c) shows that the response tends to be wideband owing to irregular motions of the panel.

Composite Panels

Panel flutter of composite plates can be studied in a similar fashion. As the first example, a simply supported square graphite/epoxy panel of eight layers [0/45/–45/90]$_s$ is investigated. The dimensions and material properties of the panel are as follows:

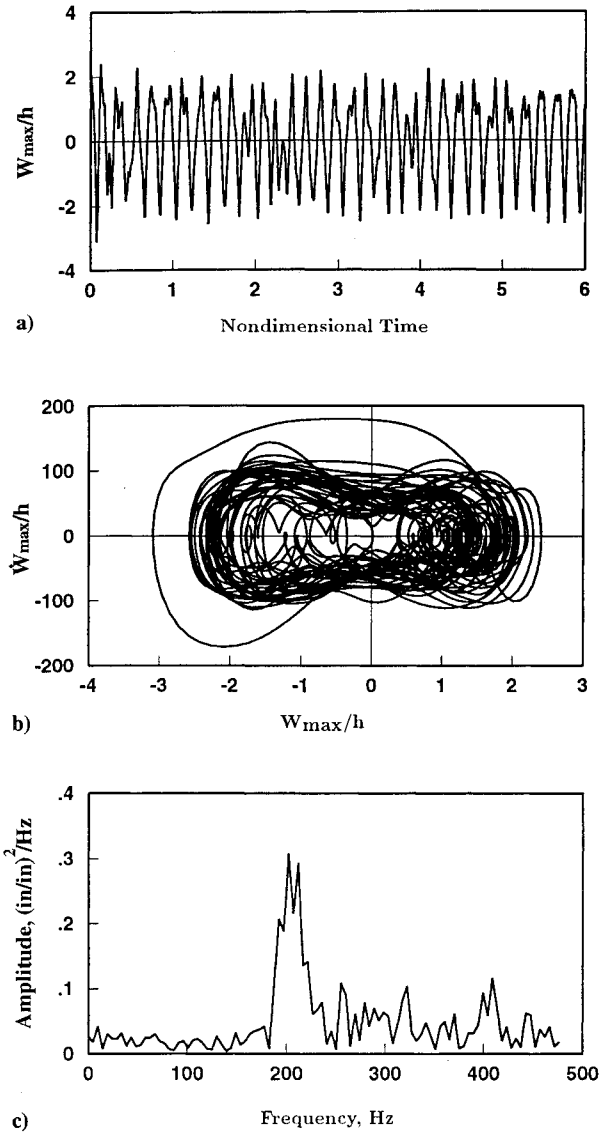

Fig. 10 Chaotic motions of a simply supported square $[0/45/-45/90]_s$ panel ($\mu/M_\infty = 0.01$) at $\lambda = 230$ and $\Delta T/\Delta T_{cr} = 6.0$.

a = 12 in. (30.5 cm)
h = 0.050 in. (0.127 cm)
E_1 = 22.5 Msi (155 GPa)
E_2 = 1.17 Msi (8.07 GPa)
G_{12} = 0.66 Msi (4.55 GPa)
ν_{12} = 0.22
α_1 = $-0.04 \times 10^{-6}/°F$ ($-0.07 \times 10^{-6}/°C$)
α_2 = $16.7 \times 10^{-6}/°F$ ($30.1 \times 10^{-6}/°C$)
ρ = 0.1458×10^{-3} lb $-$ s^2/in.^{4} (1550 kg/m^3)

The complete plate is modeled with a 10×6 mesh or 60 rectangular plate elements. The aerodynamic damping coefficient c_a is taken to be 0.01. Figure 6 studies the convergence of limit-cycle results by retaining different numbers of modes in the modal equations. It can be seen that a six-mode model will give accurate results (the same as the isotropic case). Figure 7 shows the panel deflection vs dynamic pressure at various temperatures ($\Delta T/\Delta T_{cr} = 0$, 1.0, and 2.0). The critical temperature ΔT_{cr} is 21.387°F. The higher the temperature ratio $\Delta T/\Delta T_{cr}$, the lower the dynamic pressure λ. This resembles exactly the isotropic case (cf. Fig. 2).

Figures 8a–8c illustrate the limit-cycle motions for the symmetric composite panel at $\lambda = 450$ and $\Delta T/\Delta T_{cr} = 1.0$. The harmonic behavior is clearly shown. In Figs. 9a–9c the periodic results are shown for the same composite panel at $\lambda = 140$ and $\Delta T/\Delta T_{cr} = 3.0$. At high temperature $\Delta T/\Delta T_{cr} = 6.0$ and moderate $\lambda = 230$, the panel motion shows chaotic behavior, which can be seen in Figs. 10a–10c. The phase plane plot, Fig. 10b, shows an irregular motion and the PSD, Fig. 10c, clearly verifies this.

An unsymmetric laminated ($[B] \neq 0$) square panel of two layers [0/90] is studied as well. The top is the 0-deg layer and with the airflow. The panel characterizes no bifurcation behavior due to the thermal bending moment. Thus, there is no critical temperature in this case. A reference temperature, however, is obtained by setting the thermal bending load vector to zero. For a simply supported unsymmetric square panel with the same material properties and dimensions as those of the symmetric case, this reference temperature ΔT_{ref} is found to be 16.718°F. Because of this unsymmetry, the limit-cycle motion is that the response is no longer purely harmonic, and the top and bottom panel amplitudes are not equal. Moreover, the top amplitude is slightly larger than that of the bottom. This is depicted in Fig. 11 for $\lambda = 400$ and $\Delta T/\Delta T_{ref} = 1.0$. Figures 12a–12c show the chaotic motion for this unsymmetric composite panel at $\lambda = 320$ and $\Delta T/\Delta T_{ref} = 6.0$. It is difficult to distinguish the obvious periodic motion from the chaotic region due to the effect of the coupling matrix $[B]$.

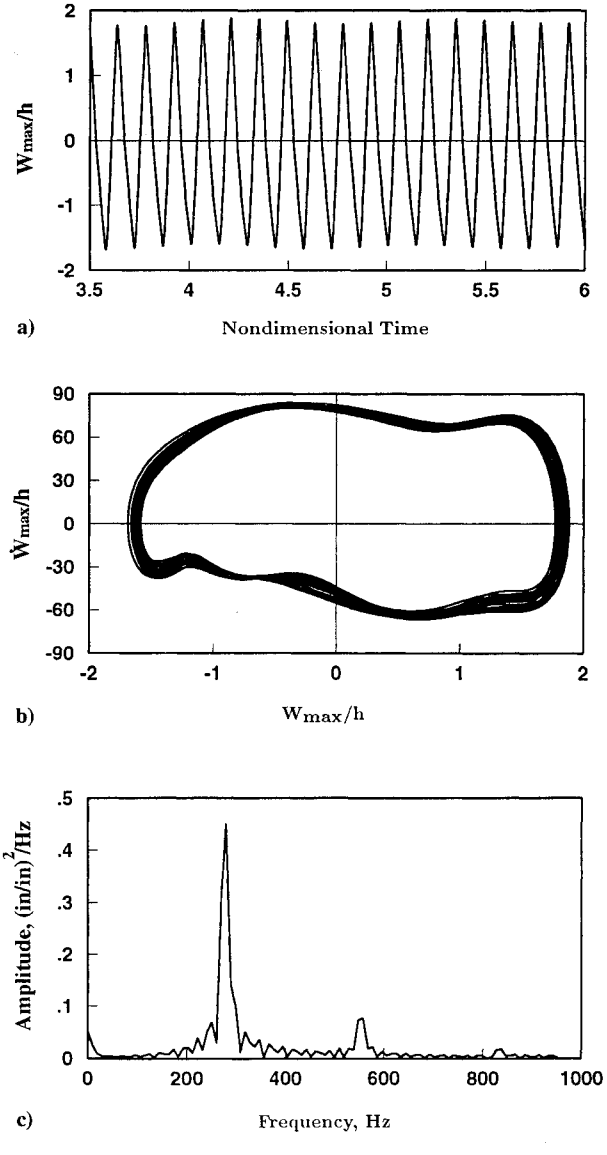

Fig. 11 Limit-cycle motions of a simply supported square [0/90] panel ($\mu/M_\infty = 0.1$) at $\lambda = 400$ and $\Delta T/\Delta T_{ref} = 1.0$.

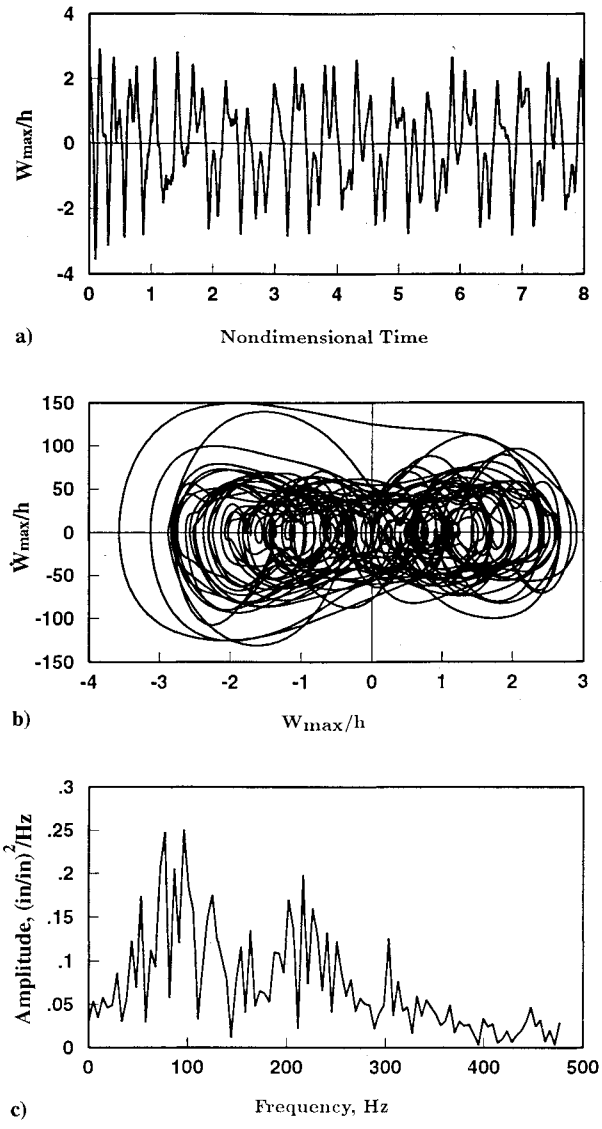

Fig. 12 Chaotic motions of a simply supported square [0/90] panel ($\mu/M_\infty = 0.1$) at $\lambda = 320$ and $\Delta T/\Delta T_{ref} = 6.0$.

Conclusions

A finite element time domain modal formulation is presented for the analysis of nonlinear flutter of composite panels at elevated temperatures. Isotropic panels can be treated as a special case of the composite panel. Six modes are needed to obtain the convergent limit-cycle results. The flutter dynamic pressure will reduce as the temperature rises. The present time domain modal method can predict all five types of panel behavior: flat, buckled, limit-cycle, periodic, and chaotic; whereas the frequency domain method fails to predict the periodic and chaotic motions. For unsymmetric composite panels undergoing limit-cycle motions, the panel amplitudes are not equal. Furthermore, due to the greatly reduced degrees of freedom in the nonlinear modal equations of motion, the present panel flutter modal formulation can be employed for flutter suppression using various active control schemes.

Appendix

For symmetrically laminated composite and isotropic panels, the laminate coupling stiffness $[B]$ is null; thus the two stiffness submatrices in Eq. (10) are

$$[K_B] = [K1_{NB}] = 0 \tag{A1}$$

By neglecting the membrane inertia term, the membrane displacement vector can be expressed in terms of the bending displacement vector as

$$\{W_m\} = [K]_m^{-1}(\{P_{\Delta T}\}_m - [K1]_{mb}\{W_b\}) \tag{A2}$$

Then Eq. (10) can be written in terms of the bending displacements as

$$\begin{aligned}&\frac{1}{\omega_0^2}[M]_b\{\ddot{W}_b\} + \frac{g_a}{\omega_0}[G]\{\dot{W}_b\}\\ &\quad + (\lambda[A_a] + [K]_b - [K_{N\Delta T}])\{W_b\}\\ &\quad + [K1]_{bm}[K]_m^{-1}\{P_{\Delta T}\}_m + [K1_{Nm}]_b\{W_b\}\\ &\quad + ([K2] - [K1]_{bm}[K]_m^{-1}[K1]_{mb})\{W_b\} = \{P_{\Delta T}\}_b\end{aligned} \tag{A3}$$

All of the system matrices in Eqs. (A1–A3) have been defined in Eq. (10).

The nonlinear stiffness matrices $[K1]_{bm}$ and $[K2]$ can be expressed in terms of the modal coordinates as

$$[K1]_{bm} = \sum_{r=1}^{n} q_r [K1]_{bm}^{(r)} \tag{A4}$$

and

$$[K2] = \sum_{r=1}^{n}\sum_{s=1}^{n} q_r q_s [K2]^{(rs)} \tag{A5}$$

The nonlinear stiffness matrix $[K1_{Nm}]_b$ is linearly dependent on the membrane displacements $\{W_m\}$ that can be expressed in terms of the modal coordinates as

$$\begin{aligned}\{W_m\} &= [K]_m^{-1}\left(\{P_{\Delta T}\}_m - \sum_{r=1}^{n}\sum_{s=1}^{n} q_r q_s [K1]_{mb}^{(r)}\{\phi_s\}_b\right)\\ &= \{W_m\}_0 + \sum_{r=1}^{n}\sum_{s=1}^{n} q_r q_s \{W_m\}_{rs}\end{aligned} \tag{A6}$$

where

$$\{W_m\}_0 = [K]_m^{-1}\{P_{\Delta T}\}_m \tag{A7}$$

$$\{W_m\}_{rs} = -[K]_m^{-1}[K1]_{mb}^{(r)}\{\phi_s\}_b \tag{A8}$$

Thus, the matrix $[K1_{Nm}]_b$ is the sum of two matrices: the first matrix $[K_{Nm}]$ is evaluated with $\{W_m\}_0$, and the second matrix $[K2_{Nm}]^{(rs)}$ is evaluated with $\{W_m\}_{rs}$ as

$$[K1_{Nm}]_b = [K_{Nm}] + \sum_{r=1}^{n}\sum_{s=1}^{n} q_r q_s [K2_{Nm}]^{(rs)} \tag{A9}$$

With the modal transformation of Eq. (24) and Eqs. (A4–A9), Eq. (A3) reduces to

$$[\bar{M}]_b\{q_{,\tau\tau}\} + [C]\{q_{,\tau}\} + ([\bar{K}]_b + [K_{qq}]_b)\{q\} = \{f\} \tag{A10}$$

where the diagonal modal mass and aerodynamic damping matrices are

$$([\bar{M}]_b, [C]) = [\Phi]^t([M_b], g_a[G])[\Phi] \tag{A11}$$

the linear terms in {q} are

$$[\bar{K}]_b\{q\} = [\Phi]^t(\lambda[A_a] + [K]_b - [K_{N\Delta T}] + [K_{Nm}])[\Phi]\{q\} + [\Phi]^t\left(\sum_{r=1}^{n} q_r[K1]_{bm}^{(r)}\{W_m\}_0\right) \quad \text{(A12)}$$

the cubic terms in {q} are

$$[K_{qq}]_b\{q\} = [\Phi]^t\left(\sum_{r=1}^{n}\sum_{s=1}^{n} q_r q_s[K2_{Nm}]^{(rs)} + \sum_{r=1}^{n}\sum_{s=1}^{n} q_r q_s[K2]^{(rs)} - \sum_{r=1}^{n}\sum_{s=1}^{n} q_r q_s[K1]_{bm}^{(r)}[K]_m^{-1}[K1]_{mb}^{(s)}\right)[\Phi]\{q\} \quad \text{(A13)}$$

and the modal thermal load vector is

$$\{f\} = [\Phi]^t\{P_{\Delta T}\}_b \quad \text{(A14)}$$

References

[1]Bisplinghoff, R. L., and Ashley, H., *Principles of Aeroelasticity*, Wiley, New York, 1962, pp. 419, 420.

[2]Baker, R., "F-117A Structures and Dynamics Design Considerations," Plenary Session 8, AIAA Dynamics Specialists Conference, Dallas, TX, April 1992.

[3]Dowell, E. H., "Panel Flutter: A Review of the Aeroelastic Stability of Plates and Shells," *AIAA Journal*, Vol. 8, No. 3, 1970, pp. 385–399.

[4]Reed, W. H., Hanson, P. W., and Alford, W. J., "Assessment of Flutter Model Testing Relating to the National Aero-Space Plane," Langley Research Center, NASP CR 1002, July 1987.

[5]Gray, C. E., Jr., and Mei, C., "Large Amplitude Finite Element Flutter Analysis of Composite Panels in Hypersonic Flow," *AIAA Journal*, Vol. 31, No. 6, 1993, pp. 1090–1099.

[6]Houbolt, J. C., "A Study of Several Aerothermoelastic Problems of Aircraft Structures in High-Speed Flight," Ph.D. Thesis, Eidenössischen Technischen Hochschule, Swiss Federal Inst. of Technology, Zurich, Switzerland, 1958.

[7]Schaeffer, H. G., and Heard, W. L., Jr., "Flutter of a Flat Plate Exposed to a Nonlinear Temperature Distribution," *AIAA Journal*, Vol. 3, No. 10, 1965, pp. 1918–1923.

[8]Yang, T. Y., and Han, A. D., "Flutter of Thermally Buckled Finite Element Panels," *AIAA Journal*, Vol. 14, No. 7, 1976, pp. 975–977.

[9]Xue, D. Y., Mei, C., and Shore, C. P., "Finite Element Two-Dimensional Panel Flutter at High Supersonic Speeds and Elevated Temperature," *Proceedings of the AIAA/ASME/ASCE/ASH/ASC 31st Structures, Structural Dynamics, and Materials Conference* (Long Beach, CA), AIAA, Washington, DC, 1990, pp. 1464–1475 (AIAA Paper 90-0982).

[10]Xue, D. Y., and Mei, C., "Finite Element Nonlinear Flutter and Fatigue Life of Two-Dimensional Panels with Temperature Effects," *Proceedings of the AIAA/ASME/ASCE/AHS/ASC 32nd Structures, Structural Dynamics, and Materials Conference* (Baltimore, MD), AIAA, Washington, DC, 1991, pp. 1981–1991 (AIAA Paper 91-1170); also *Journal of Aircraft*, Vol. 30. No. 6, 1993, pp. 993–1000.

[11]Xue, D. Y., and Mei, C., "Finite Element Nonlinear Panel Flutter with Arbitrary Temperatures in Supersonic Flow," *AIAA Journal*, Vol. 31, No. 1, 1993, pp. 154–162.

[12]Dixon, I. R., and Mei, C., "Nonlinear Flutter of Rectangular Composite Panels Under Uniform Temperature Using Finite Elements," *Nonlinear Vibrations*, edited by R. A. Ibrahim, N. S. Namachchivaya, and A. K. Bajaj, ASME DE-Vol. 50, ASME Winter Annual Meeting, American Society of Mechanical Engineers, New York, Nov. 1992, pp. 123–132.

[13]Dowell, E. H., "Nonlinear Oscillations of a Fluttering Plate," *AIAA Journal*, Vol. 4, No. 7, 1966, pp. 1267–1275.

[14]Han, A. D., and Yang, T. Y., "Nonlinear Panel Flutter Using High-Order Triangular Finite Elements," *AIAA Journal*, Vol. 21, No. 10, 1983, pp. 1453–1461.

[15]Qin, J., Gray, C. E., Jr., and Mei, C., "A Vector Unsymmetric Eigenequation Solver for Nonlinear Flutter Analysis on High-Performance Computers," *Journal of Aircraft*, Vol. 30, No. 5, 1993, pp. 744–750.